Gravitational wave data analysis implications of TaylorEt inspiral approximants for ground-based detectors: the non-spinning case

Sukanta Bose*
Department of Physics & Astronomy, Washington State University, 1245 Webster, Pullman, WA 99164-2814, U.S.A. †

Achamveedu Gopakumar‡ and Manuel Tessmer§
Theoretisch-Physikalisches Institut, Friedrich-Schiller-Universität Jena, Max-Wien-Platz 1,07743 Jena, Germany‡

(Dated: July 15, 2008; LIGO Document Control Center No. LIGO-T080142-00-Z)

A new family of restricted post-Newtonian-accurate waveforms, termed TaylorEt approximants, was recently proposed for searching gravitational wave (GW) signals from inspiraling non-spinning compact binaries having arbitrary mass-ratios. One of the attractive features exhibited by these waveforms is that as their reactive post-Newtonian (PN) order is increased, their phase-evolution monotonically converges to that of waveforms produced by numerical relativity. The TaylorEt approximant is different from the usual post-Newtonian ones, such as the TaylorT1, TaylorT4, and TaylorF2 approximants, in that it gives equal emphasis to both the conservative and the reactive parts of GW phase evolution. However, for the latter set of extensively employed PN-accurate inspiral templates the conservative phase evolution is somewhat dwarfed by the reactive part. We perform detailed fitting factor (FF) studies to probe if the TaylorEt (3.5PN) signals for non-spinning comparable mass compact binaries can be effectually and faithfully searched with TaylorT1, TaylorT4, and TaylorF2 (3.5PN) templates in LIGO, Advanced LIGO, and Virgo interferometers. We observe that a good fraction of the templates, which by choice are from TaylorT1, TaylorT4, and TaylorF2 (3.5PN) families, have FF $\lesssim 0.97$ and substantial biases for the estimated total-mass against the fiducial TaylorEt (3.5PN) signals for equal-mass systems. Both these observations can bear on the detectability of a signal. TaylorEt (3.5PN) signals with mass-ratios of a third or a quarter yield high FFs against those same template banks, but at the expense of inviting large systematic errors in the estimated values of their total mass and symmetric mass-ratio. In general, the aforementioned templates are found to be increasingly *unfaithful* with respect to a TaylorEt signal as one increases the total mass of the inspiraling system. We find that one way of improving the FF values is to allow the templates to have unphysical mass-ratios. However, this may result in a higher noise background and, therefore, reduce the detection confidence. We also observe that the amount of bias in the estimated mass varies with the (noise power spectral density of the) detector. This can be of some concern for multi-detector searches, which check for consistency in the estimated masses of concurrent triggers in their data. However, by modeling this variation it is possible to mitigate its effect on the detection efficiency.

PACS numbers: 04.30.Db, 04.25.Nx 04.80.Nn, 97.60.Jd, 95.55Ym

arXiv:0807.2400v2 [gr-qc] 28 Feb 2012

I. INTRODUCTION

Stellar mass compact binaries, involving black holes and neutron stars, are the most promising sources of gravitational radiation for the operational and planned ground-based laser interferometric gravitational wave (GW) detectors. Gravitational wave signals from inspiraling compact binaries are being searched in the detector data by using *matched filtering* [1] with several types of theoretically modeled inspiral templates [2, 3]. A good resource for computing these templates in software, which is being actively used by the LIGO Scientific Collaboration (LSC) [4] and the Virgo Collaboration [5] for analyzing detector data, is the LSC Algorithm Library (LAL) [6].

As such, the construction of these search templates requires *two* crucial inputs from the post-Newtonian (PN) approximation to general relativity, appropriate for describing the dynamics of a compact binary during its inspiral phase. These are the 3PN accurate dynamical (orbital) energy $\mathcal{E}(x)$ and the 3.5PN accurate expression for the GW luminosity $\mathcal{L}(x)$ [7], both of which are usually expressed as PN series in the gauge invariant quantity $x \equiv (G\,m\,\omega/c^3)^{2/3}$, where m and ω are the total mass and the orbital angular frequency of the binary, and the familiar symbols G and c denote the universal gravitational constant and the speed of light in vacuum, respectively. Recall that the 3PN accurate expression for $\mathcal{E}(x)$ provides corrections to the Newtonian orbital energy to the order of $(v/c)^6$, where v is the orbital speed. Further, the currently employed search templates only require the Newtonian contributions to the amplitude of GW polarizations, $h_+(t)$ and $h_\times(t)$. However, expressions for $h_+(t)$

*Electronic address: sukanta@wsu.edu
†Currently at *Max-Planck-Institut für Gravitationsphysik, Albert-Einstein-Institut, Callinstr. 38, 30167 Hannover, Germany*
‡Electronic address: a.gopakumar@uni-jena.de
§Electronic address: m.tessmer@uni-jena.de

and $h_\times(t)$ that include the 3PN amplitude corrections are available in Ref. [8] and are being used to develop amplitude corrected templates for GW inspiral searches.

With the help of the two aforesaid PN-accurate inputs, one can construct two distinct classes of inspiral GW templates. The templates belonging to the first category require

$$\frac{d\phi(t)}{dt} = \omega(t) \equiv \frac{c^3}{G\,m}\,x^{3/2} \tag{1}$$

and PN-accurate prescriptions for the reactive evolution of $x(t)$. Such templates are usually referred to as *adiabatic* inspiral templates, and all PN-accurate inspiral templates that LAL employs are of this type. In this paper, we consider from this class time-domain templates of the TaylorT1 [7] and the Numerical Relativity (NR) inspired TaylorT4 [9] families and frequency-domain templates of the TaylorF2 family [15]. For all three families, we incorporate radiation reaction effects to the (relative) 3.5PN order (see Eqs. (2), (4), and (6) below). Due to their use of the x-based phase evolution expression in Eq. (1), it may be argued that these templates model GWs from compact binaries inspiraling under PN-accurate radiation reaction along *exact* circular orbits [10].

A new class of inspiral approximants introduced in Ref. [10], termed as TaylorEt, requires PN expansion for $d\phi/dt$ in terms of the orbital binding *Energy* to derive the *temporal* GW phase evolution. This alternative phasing prescription models GWs from compact binaries inspiraling under PN-accurate reactive dynamics along *PN-accurate circular orbits* [10]. In other words, the TaylorEt approximant *explicitly* incorporates the secular contributions to GW phase evolution appearing at the 1PN, 2PN, and 3PN orders. Contrastingly, in the case of x-based adiabatic inspiral templates and due to the use of Eq. (1), the above mentioned conservative (and secular) contributions to the GW phase evolution do not appear before the radiation reaction kicks in at the absolute 2.5PN order. It should be noted that the cost of computing TaylorEt templates is comparable to that of TaylorT1/T4 templates.

In this paper, we study how effectively and faithfully the TaylorT1, TaylorT4, and TaylorF2 inspiral templates, at 3.5PN order, can capture a GW signal modeled using the TaylorEt approximant of the same order. The main motivation for using the latter as the fiducial signal originates from the observation that the TaylorEt approximant is an appropriate zero-eccentricity limit of GW phasing for compact binaries inspiraling along PN-accurate eccentric orbits [10]. We quantify our results by computing fitting factors (FF) following prescriptions detailed in Refs. [11, 12], and inherent systematic errors in the estimated value of m and the symmetric mass-ratio, η, for the various search templates, relevant for the initial LIGO (heretofore referred to as "LIGO"), Advanced LIGO (or "AdLIGO") and Virgo detectors. We conclude that it is desirable to incorporate the TaylorEt approximant at 3.5PN order into LAL to minimize possible loss of inspiral events. Further, one might also view this work as an exercise in assessing the effects of using inspiral templates from different representations on a GW signal's detectability and parameter estimation in earth-based detectors. Similar assessments of systematic errors on GW searches in LISA and Virgo were made by comparing inspiral templates of different PN orders from the same representation in Refs. [13] and [14], respectively.

The plan of the paper is as follows. In the next section, Sec. II, we provide explicit PN-accurate equations required for constructing TaylorT1, TaylorT4, TaylorF2 and TaylorEt templates having 3.5PN accurate reactive evolution. Section III explains how we perform our FF computations and tabulates their values, along with the associated systematic errors in m and η, for our different templates. We briefly discuss the implications of these results on the on-going searches in real interferometric data. We conclude in Sec. IV by providing a brief summary and future directions.

II. PHASING FORMULAE FOR VARIOUS INSPIRAL TEMPLATES

The PN approximation to general relativity is expected to describe accurately the adiabatic inspiral phase of a comparable mass compact binary [9]. During this phase, the change in the orbital frequency over one orbit may be considered to be tiny compared to the mean orbital frequency itself. For compact binaries, having negligible eccentricities, the adiabatic orbital phase evolution can be accurately described with the help of 3PN and 3.5PN accurate expressions for the orbital energy and the GW luminosity, respectively, available in Refs. [7]. While employing x as a PN expansion parameter, there exist several prescriptions to compute the adiabatic GW phase evolution. Each prescription, termed a PN approximant, provides a slightly different GW phase evolution and, correspondingly, a different inspiral template family. Following Ref. [6], we first list the equations describing the TaylorT1 and the TaylorF2 approximants, which are regularly employed by various GW data analysis groups. The time-domain TaylorT1 approximant is given by

$$h(t) \propto x\,\cos 2\,\phi(t)\,, \tag{2a}$$

$$\frac{d\phi(t)}{dt} = \omega(t) \equiv \frac{c^3}{G\,m}\,x^{3/2}\,, \tag{2b}$$

$$\frac{d\,x(t)}{dt} = -\frac{\mathcal{L}(x)}{(d\mathcal{E}/dx)}\,, \tag{2c}$$

where the proportionality constant in Eq. (2a) may be set to unity for our analysis. To construct the TaylorT1 3.5PN order adiabatic inspiral templates, one needs to use 3.5PN accurate $\mathcal{L}(x)$ and 3PN accurate $\mathcal{E}(x)$, respectively. The explicit expressions for these quantities, ex-

tracted from Refs. [7], read

$$\mathcal{L}(x) = \frac{32\,\eta^2\,c^5}{5\,G}\,x^5\left\{1-\left[\frac{1247}{336}+\frac{35}{12}\,\eta\right]x+4\,\pi\,x^{3/2} - \left[\frac{44711}{9072}-\frac{9271}{504}\,\eta-\frac{65}{18}\,\eta^2\right]x^2-\left[\frac{8191}{672} + \frac{583}{24}\,\eta\right]\pi\,x^{5/2}+\left[\frac{6643739519}{69854400}+\frac{16\,\pi^2}{3} - \frac{1712}{105}\,\gamma-\left(\frac{134543}{7776}-\frac{41}{48}\,\pi^2\right)\eta-\frac{94403}{3024}\,\eta^2 - \frac{775}{324}\,\eta^3-\frac{1712}{105}\,\ln\left(4\,\sqrt{x}\right)\right]x^3-\left[\frac{16285}{504} - \frac{214745}{1728}\,\eta-\frac{193385}{3024}\,\eta^2\right]\pi\,x^{7/2}\right\}, \tag{3a}$$

$$\mathcal{E}(x) = -\frac{\eta\,m\,c^2}{2}\,x\left\{1-\frac{1}{12}\left[9+\eta\right]x-\left[\frac{27}{8}-\frac{19}{8}\,\eta + \frac{1}{24}\,\eta^2\right]x^2-\left[\frac{675}{64}+\frac{35}{5184}\,\eta^3+\frac{155}{96}\,\eta^2 + \left(\frac{205}{96}\,\pi^2-\frac{34445}{576}\right)\eta\right]x^3\right\}, \tag{3b}$$

where γ is the Euler constant and $\eta \equiv \mu/m$, with μ being the reduced mass of the binary.

The frequency-domain TaylorF2 approximant at 3.5PN order, extracted from Ref. [15], reads

$$\tilde{h}(f) \propto f^{-7/6}\,e^{i\,\psi(f)}\,, \tag{4a}$$

$$\psi(f) = 2\,\pi\,f\,t_c-\phi_c-\frac{\pi}{4} + \frac{3}{128\,\eta\,(v/c)^5}\sum_{k=0}^{k=7}\alpha_k\,\left(\frac{v}{c}\right)^k\,, \tag{4b}$$

where $v = (G\pi\,m\,f/c^3)^{1/3}$, and t_c and ϕ_c are the fiducial time and phase of coalescence, respectively. The explicit expressions for the PN coefficients α_k are

$$\alpha_0 = 1, \tag{5a}$$

$$\alpha_1 = 0, \tag{5b}$$

$$\alpha_2 = \frac{20}{9}\,\left(\frac{743}{336}+\frac{11}{4}\eta\right), \tag{5c}$$

$$\alpha_3 = -16\pi, \tag{5d}$$

$$\alpha_4 = 10\,\left(\frac{3058673}{1016064}+\frac{5429}{1008}\,\eta+\frac{617}{144}\,\eta^2\right), \tag{5e}$$

$$\alpha_5 = \pi\left\{\frac{38645}{756}+\frac{38645}{252}\,\log\left(\frac{v}{v_{\rm lso}}\right) - \frac{65}{9}\eta\left[1+3\log\left(\frac{v}{v_{\rm lso}}\right)\right]\right\}, \tag{5f}$$

$$\alpha_6 = \left(\frac{11583231236531}{4694215680}-\frac{640\,\pi^2}{3}-\frac{6848\,\gamma}{21}\right) - \eta\left(\frac{15737765\,635}{3048192}-\frac{2255\,\pi^2}{12}\right) + \frac{76055}{1728}\eta^2-\frac{127825}{1296}\eta^3-\frac{6848}{21}\log\left(4\,v\right), \tag{5g}$$

$$\alpha_7 = \left(\frac{77096675}{254016}+\frac{378515}{1512}\,\eta-\frac{74045}{756}\,\eta^2\right)\,\pi\,, \tag{5h}$$

where $v_{\rm lso}$ is the speed at the last stable orbit, which we take to be at $6\,Gm/c^2$.

Recently, Ref. [9] introduced another Taylor approximant, termed TaylorT4. This approximant is obtained by Taylor expanding in x the right-hand side of Eq. (2c) for dx/dt and truncating it at the appropriate reactive PN order. This approximant at 3.5PN order has an interesting (and accidental) property that was discovered due to the recent advances in Numerical Relativity (NR) involving coalescing binary black holes [16]. It was observed in Ref. [9] that the NR-based GW phase evolution for an equal-mass binary black hole agrees quite well with its counterpart in TaylorT4 approximant at 3.5PN order. Specifically, Ref. [9] observed that the accumulated GW phase difference between TaylorT4 waveforms at 3.5PN order and NR waveforms agrees within 0.06 radians over 30 wave cycles and matched at $x \sim 0.215$. The time-domain TaylorT4 approximant at 3.5PN order is specified by

$$h(t) \propto x\,\cos 2\,\phi(t)\,, \tag{6a}$$

$$\frac{d\phi(t)}{dt} = \omega(t) \equiv \frac{c^3}{G\,m}\,x^{3/2}\,, \tag{6b}$$

$$\frac{d\,x(t)}{dt} = \frac{c^3}{G\,m}\,\frac{64\,\eta}{5}\,x^5\left\{1-\left(\frac{743}{336}+\frac{11}{4}\,\eta\right)x+4\,\pi\,x^{3/2} + \left(\frac{34103}{18144}+\frac{13661}{2016}\,\eta+\frac{59}{18}\,\eta^2\right)x^2-\left[\frac{4159}{672} + \frac{189}{8}\,\eta\right]\pi\,x^{5/2}+\left[\frac{16447322263}{139708800}-\frac{1712}{105}\,\gamma + \frac{16\,\pi^2}{3}-\frac{3424}{105}\,\ln\left(2\right)-\frac{856}{105}\,\ln\left(x\right)-\left(\frac{56198689}{217728} - \frac{451}{48}\,\pi^2\right)\eta+\frac{541}{896}\,\eta^2-\frac{5605}{2592}\,\eta^3\right]x^3-\left[\frac{4415}{4032} - \frac{358675}{6048}\,\eta-\frac{91495}{1512}\,\eta^2\right]\pi\,x^{7/2}\right\}. \tag{6c}$$

It should be noted that the TaylorF2 waveform in Eqs. (4) is the Fourier transform of $h(t)$, given by Eqs. (6) above, computed with the help of the stationary phase approximation [17]; we speculate that this is the reason that the TaylorT4 approximant is not directly employed in LAL (which already uses the TaylorF2 approximant).

A close inspection of various time-domain adiabatic inspiral templates available in LAL reveals that they all invoke Eq. (1). These template families are different from one another only in the manner in which they incorporate the reactive evolution of $x(t)$. For example, PadeT1 time-domain inspiral templates are constructed by invoking a specific Pade resummation for the right-hand side of Eq. (6c). Therefore, we may state that various x-based inspiral templates provide slightly different

GW phase evolution by perturbing a compact binary in an exact circular orbit, defined by Eq. (1), by different prescriptions for the reactive evolution of $x(t)$. This is the main reason behind the observation that these templates model GWs from compact binaries inspiraling under PN-accurate radiation reaction along *exact* circular orbits.

Interestingly, it is possible to construct, in a gauge-invariant manner, inspiral GW search templates that do not require working in terms of the x variable. The TaylorEt approximant [10] employs the orbital binding energy in lieu of that variable to describe PN-accurate adiabatic GW phase evolution. Hence, it requires an appropriate PN expansion for $d\phi/dt$ in terms of the orbital binding energy. Accordingly, it can be argued that the TaylorEt approximant models GWs from compact binaries inspiraling under PN-accurate radiation reaction along *PN-accurate circular orbits*.

The TaylorEt approximant at 3.5PN order is defined by

$$h(t) \propto \mathcal{E}(t)\, \cos 2\,\phi(t)\,, \tag{7a}$$

$$\begin{aligned}\frac{d\phi(t)}{dt} \equiv \omega(t) = \frac{c^3}{G\,m}\,\xi^{3/2}\Bigg\{1 + \frac{1}{8}\,(9+\eta)\,\xi + \Bigg[\frac{891}{128} \\ - \frac{201}{64}\,\eta + \frac{11}{128}\,\eta^2\Bigg]\xi^2 + \Bigg[\frac{41445}{1024} - \Bigg(\frac{309715}{3072} \\ - \frac{205}{64}\,\pi^2\Bigg)\eta + \frac{1215}{1024}\,\eta^2 + \frac{45}{1024}\,\eta^3\Bigg]\xi^3\Bigg\}\,,\end{aligned} \tag{7b}$$

$$\begin{aligned}\frac{d\,\xi(t)}{dt} = \frac{64}{5}\,\eta\,\xi^5\Bigg\{1 + \left(\frac{13}{336} - \frac{5}{2}\,\eta\right)\xi + 4\,\pi\,\xi^{3/2} \\ + \left(\frac{117857}{18144} - \frac{12017}{2016}\,\eta + \frac{5}{2}\,\eta^2\right)\xi^2 + \Bigg[\frac{4913}{672} \\ - \frac{177}{8}\,\eta\Bigg]\,\pi\,\xi^{5/2} + \Bigg[\frac{37999588601}{279417600} \\ - \frac{1712}{105}\,\ln\left(4\,\sqrt{\xi}\right) - \frac{1712}{105}\,\gamma + \frac{16\,\pi^2}{3} \\ + \left(\frac{369}{32}\,\pi^2 - \frac{24861497}{72576}\right)\eta + \frac{488849}{16128}\,\eta^2 \\ - \frac{85}{64}\,\eta^3\Bigg]\xi^3 + \Bigg[\frac{129817}{2304} - \frac{3207739}{48384}\,\eta \\ + \frac{613373}{12096}\,\eta^2\Bigg]\,\pi\,\xi^{7/2}\Bigg\}\,,\end{aligned} \tag{7c}$$

where $\xi = -2\,\mathcal{E}/\mu\,c^2$. A close inspection of Eqs. (7) reveals that the above inspiral $h(t)$ is obtained by perturbing a compact binary in a 3PN accurate circular orbit, defined by Eq. (7b), by radiation reaction effects at 3.5PN order, given by Eq. (7c). The explicit use of PN-accurate expression for $d\phi/dt$ allows us to state that the TaylorEt approximants model GWs from compact binaries inspiralling under PN accurate reactive dynamics along PN accurate circular orbits.

Importantly, a recent study of the accumulated phase difference between NR waveforms on the one hand and TaylorEt, TaylorT1, and TaylorT4 waveforms on the other hand reveals the following characteristics [18]. In the interval $x \sim 0.127$ to $x \sim 0.215$ this difference for the TaylorEt approximant at 3.5PN order is $\delta\phi \sim -1.18$ radians, which is more than what is found for the TaylorT1 and TaylorT4 counterparts (with $\delta\phi \sim 0.6$ and 0.06 radians, respectively). However, significantly, TaylorEt is the only approximant studied so far that exhibits monotonic phase convergence with the NR waveforms when its reactive PN order is increased [18]. Recall that sophisticated Padé approximations are required to make x-based Taylor approximants converge monotonically to the $h(t)$ obtained from numerical relativity in the $\eta = 0$ case [12]. In the context of the present paper, the analysis detailed in Ref. [18] also suggests that TaylorEt approximant at 3.5PN order remains fairly accurate in describing the inspiral $h(t)$ even near the last stable orbit. These properties make it worthwhile to study the data analysis implications of TaylorEt approximants.

Another motivation for using the TaylorEt approximant to model the expected inspiral GW signal is as follows: With the help of Refs. [10, 19], it can be argued that TaylorEt is an appropriate approximant resulting from the zero-eccentricity limit of GW phasing of compact binaries inspiraling along PN-accurate eccentric orbits. By contrast, the construction of the usual *adiabatic* inspiral templates requires redefining the right-hand side of Eq. (7b) to be $c^3x^{3/2}/Gm$, which can not be extended to yield GWs from precessing and inspiraling eccentric binaries as obtained in Ref. [19]. Therefore, the TaylorEt approximant can be expected to closely model GW signals from inspiraling compact binaries, which realistically will not move along exactly circular orbits. The above statements are based on Ref. [20] that, while restricting radiation reaction to the dominant quadrupole contributions, demonstrated the undesirable consequences of redefining the right-hand side of Eq. (7b) at 2PN order to be $c^3x^{3/2}/Gm$.

Currently, for the low-mass binary signal searches the LSC usually employs templates based on TaylorTn (where n=1, 2, and 3) and TaylorF2 approximants [6, 27]. Therefore, it is important to probe if some of these templates can capture inspiral signals modeled on the TaylorEt approximant. This is what we pursue in the next section.

III. FITTING FACTORS

Inspiraling compact binaries are the most promising sources of GWs for LIGO/Virgo. Detailed source population synthesis studies suggest that achieving an appreciable event rate, of at least a few compact binary coalescences per year, is possible if one could hear sources in the far reaches of our local super-cluster and beyond [21, 22]. Such an endeavor necessitates the ability to detect signals with relatively low signal-to-noise ratios (SNRs), even with second generation detectors, such as AdLIGO. Let the GW strain from a non-spinning com-

pact binary be denoted by $h(t;\boldsymbol{\lambda})$, where $\boldsymbol{\lambda}$ represents the signal parameters, namely, m, η, t_c, and ϕ_c, or an alternative set of transformed coordinates in that parameter space. If a detector's strain-data is denoted by $s(t)$ and its noise power-spectral-density (PSD) by $S_n(f)$, then the SNR when filtering the data with template $h(t;\boldsymbol{\lambda'})$ is

$$\mathrm{SNR} = \frac{\langle s|h(\boldsymbol{\lambda'})\rangle}{\sqrt{\langle h(\boldsymbol{\lambda'})|h(\boldsymbol{\lambda'})\rangle}}\,, \tag{8}$$

where $\boldsymbol{\lambda'}$ symbolizes the template parameters, which need not be the same as the parameters of a signal embedded in the data, and the inner product $\langle a|b\rangle$ is defined as,

$$\langle a|b\rangle \equiv 4\Re\int_0^\infty \frac{\tilde{a}^*(f)\tilde{b}(f)}{S_n(f)}\,df\,. \tag{9}$$

Above, $\tilde{a}(f)$ is the Fourier transform of $a(t)$ and the asterisk denotes complex conjugation. Using Eq. (8), it can be shown that the quantity

$$\mathrm{M}\,(\boldsymbol{\lambda},\boldsymbol{\lambda'}) = \frac{\langle g(\boldsymbol{\lambda})|h(\boldsymbol{\lambda'})\rangle}{\sqrt{\langle g(\boldsymbol{\lambda})|g(\boldsymbol{\lambda})\rangle\langle h(\boldsymbol{\lambda'})|h(\boldsymbol{\lambda'})\rangle}}\,, \tag{10}$$

also known as the "match", is useful in describing how well two normalized waveforms, not necessarily from the same template family, overlap [23].

For the problem of detecting a GW inspiral signal, the prevailing sentiment in the community is that it is not as essential to search with a template bank that is an exact representation of the signal, as it is to search with an approximate one that can filter the data in real-time, provided its expected maximal match with a signal from anywhere in the parameter space is above a desired threshold. In other words, it should be possible to obtain a sufficiently large 'match' with a family of templates having $\boldsymbol{\lambda'} \neq \boldsymbol{\lambda}$. It is often stressed that this faithlessness of a template in accessing the signal parameters does not concern the detection problem *per se*, but that it affects the parameter-estimation problem, which can be tackled *a posteriori*, i.e., after the transient signal has been detected and localized in time. The effectiveness of a template family, say, $h(\boldsymbol{\lambda'})$, in detecting the target signal $g(\boldsymbol{\lambda})$ is quantified by the fitting factor (FF) [11]

$$\mathrm{FF}(\boldsymbol{\lambda}) = \max_{\boldsymbol{\lambda'}} \mathrm{M}\,(\boldsymbol{\lambda},\boldsymbol{\lambda'})\,. \tag{11}$$

If a template bank provides near-unity FF values for a given signal, it is considered to be *effectual* in detecting it [12].

Employing an approximate template bank results in a drop in event rate by $(1-\mathrm{FF}^3)$ for a homogeneous distribution of sources. This is easily seen when one realizes that the FF is a measure of the fractional loss in SNR (which scales inversely with source distance) stemming from using such a bank. So, e.g., a FF of 90% results in a 27% loss in event rate in any given detector. The expected rate in LIGO or Enhanced LIGO, which is a proposed upgrade in sensitivity of LIGO by roughly a factor of two while making minimal changes to the shape of the LIGO noise PSD [24], is very low, i.e., realistically, less than one event in a few years. Therefore, a FF of 90% can potentially subvert a detection in the era of first-generation detectors. This is why a FF $\geq$ 97% is so desirable.

The values of the fitting factors for a couple of template banks against the TaylorEt 3.5PN waveforms are given in Tables II, III, and IV. The FFs were computed using two separate codes. One of these employs LAL [6], which is used by the LSC in its inspiral searches, and the other is a home-grown code that extensively uses routines from *Numerical Recipes* [25]. Both codes have the ability to compute the FF in Eq. (11) as well as the more conservative (or lower) *minimax* match, detailed in Ref. [12]. The latter is obtained by minimizing the FF of Eq. (11) with respect to the coalescence phase of the target waveform. The numbers presented in the tables are FFs (and not minimax matches) and, therefore, are larger than values that are realistically achievable with the above listed inspiral template banks, available in LAL, and the TaylorT4 template bank.

Importantly, the first few detections will likely require validation from more than one detector, which implies that in addition to being effectual a template bank also must be *faithful* [12]. The latter requirement means that the parameter values of the best matched template are allowed to differ from (a subset of) those of the signal only by acceptably small biases. This is because unless these systematics are modeled for, the same signal can be picked up by templates with parameter values different enough in two (or more) detectors so as to fail a parameter-value coincidence test [26]. We infer that differences in the estimated masses, illustrated in Tables I -IV, between different comparable class detectors, such as AdLIGO and Virgo, are due to their different noise PSDs.

Based on the tables and figures presented here, a few observations are in order. First, a good fraction of equal-mass compact binary templates, which are chosen to be from TaylorT1, TaylorT4 (presented only in the figures), and TaylorF2 (presented only in the tables) 3.5PN families, have FF $\lesssim$ 0.97. They also show substantial biases for the estimated total-mass against TaylorEt (3.5PN) signals as long as the symmetric mass-ratio of templates is limited to $\eta' \leq 0.25$, which is the upper-limit for physical signals. Note how in the first row of plots in Fig. 2 the FF first decreases as m is increased before recovering to higher values eventually. This behavior can be explained by the fact that in any given signal band the TaylorEt approximant has a greater number of GW cycles than the x-based templates of the same mass system. This means that x-based templates with $m' < m$ and $\eta' > \eta$ are more likely to provide a higher match than the one with $m' = m$ and $\eta' = \eta$. However, since for the equal-mass signals in Table II and Fig. 2 we restrict the templates to have $\eta' \leq 0.25$, the templates yielding the highest match

saturate this bound and attain $\eta' = \eta = 0.25$. This wave-based argument alone also implies that the highest match will decrease with increasing m. This is because while decreasing m' increases the number of template cycles, which helps in improving the match, decreasing it too much adversely affects the match by lowering the template $f_{\rm lso}$ and, thereby, decreasing the integration band. The reason why the FF values eventually regain high values at large m is that there the number of wave cycles is small and it is easier to obtain larger fits on signals with a smaller number of time-frequency bins.

Compact binaries with mass-ratios smaller than unity can yield high FFs, but at the expense of introducing high systematic errors in estimating the values of m and η. The high FFs can be explained by the fact that unlike in the case of equal-mass signals, here η' can exceed η, simply because $\eta < 0.25$. For illustration purposes, we consider signals with two different values of the mass-ratio, namely, $q \equiv m_1/m_2 = 1/3$ and $1/4$. In general, our inspiral templates are found to be fairly *unfaithful* with respect to the fiducial signal for these cases. Moreover, Tables II and Fig. 1 show that the TaylorT1 template with the maximum match almost always has $\eta' = 0.25$. This arises from restricting the template banks to have physical values of the symmetric mass-ratio, namely, $\eta' \leq 0.25$. As shown in Fig. 1, this can be seen from the fact that the match in Eq. (10), also known as the ambiguity function in this context, has a sharp wedge that rises with increasing η' and attains its maximum beyond $\eta' = 0.25$.

The above observation prompted us to compute FFs in Tables V with $\eta' > 0.25$. We find that it requires η' to be as high as 0.35 for the FF to attain values at least equal to 97% for the total-mass range considered here (i.e., $m \leq 40M_\odot$), albeit, at the cost of large biases in the estimated values of both m' (up to almost 20%) and η' (up to about 40%). In our opinion, while this allowance increases the match, it does not necessarily translate into an increase in the detection confidence. This is because an expanded range in η' has the potential to increase the false-alarm rate. To test what the effective gain is it is imperative to include templates with $\eta' > 0.25$ in signal simulation studies involving real interferometric data.

As presented in Tables II-III, the systematic errors also show variation with respect to the shape of the detector noise power spectral density. This implies, e.g., that the estimated value of the total mass of a signal in LIGO and Virgo can disagree and, consequently, fail a sufficiently stringent mass-consistency check in a multi-detector search [27, 28]. To wit, in the search for inspiral signals in LIGO data from its third and fourth science runs by the LSC, the estimated chirp-mass, $\mathcal{M}_c$, in the three LIGO detectors was allowed to differ by $0.020M_\odot$. A comparison of the estimated total-mass values in Tables II shows that this window needs to be relaxed if the search involved both LIGO and Virgo detectors and if TaylorEt was indeed a more appropriate representation of a GW signal. For instance, Table II shows that for $m = 5.0\ M_\odot$ the measured m' in LIGO and Virgo are expected to differ by as much as $0.062M_\odot$, which amounts to $\Delta\mathcal{M}_c = 0.026M_\odot$ (where we assumed, conservatively, that all the error in $\mathcal{M}_c$ arose from the error in m'). This is larger than the allowed window and can, therefore, fail a multi-detector mass-consistency test. The biases shown in Tables II only get worse as the total mass of the signal is increased. Note that this exercise is meant to serve as a guide for sources of systematic effects and how to deal with them; it is not clear if a concurrent search with LIGO and Virgo detectors with LIGO and Virgo design sensitivity curves, respectively, (as used for Table II) is likely. (Nevertheless, it is more likely that the shapes of the respective curves are maintained in the next set of science runs, such as with the planned Enhanced-LIGO design. This is because the FFs depend on the shape of these curves and not the overall scale). It is possible, however, to use our studies to model the variation of the estimated parameter bias in real detector data so that the windows can be scaled and shifted appropriately to mitigate the effect on detection efficiency.

IV. CONCLUSIONS

In this paper, we investigated the GW data analysis implications of the TaylorEt approximant at the 3.5PN order. We limited our attention to the case of GW signals from non-spinning, comparable mass, compact binaries in LIGO, AdLIGO and Virgo interferometers. With the help of detailed fitting factor computations, we compared the performance of three x-based inspiral templates, namely, TaylorT1, TaylorT4, and TaylorF2 at 3.5PN order, in detecting a fiducial TaylorEt signal of the same PN order. For the equal-mass binaries, we generally obtain FF $\lesssim 0.97$ when restricting the above templates to physically allowed mass-ratios. In the case of unequal mass binaries, it is possible to obtain high FFs with the LAL inspiral templates. However, the templates that provide those high FFs have substantially different values of m and η compared to those of the fiducial TaylorEt signals. In all cases, templates giving high FFs have lower values of the total-mass parameter compared to their associated TaylorEt signals. This is due to the fact that in a given GW frequency band the TaylorEt approximant always provides more accumulated GW cycles than the x-based templates. Further, the systematic errors in m and η parameters of TaylorF2 templates are substantially higher than the statistical errors in those parameters reported in Ref. [15]. These observations lead us to believe that the unfaithful nature of the x-based inspiral templates vis à vis the TaylorEt approximant may adversely affect the chances of detecting GW inspiral signals assuming that the latter waveforms more accurately represent such a signal.

To summarize, the present study shows that it should be worthwhile to include the theoretically motivated TaylorEt templates, which has a number of attractive features as detailed in Ref. [10], in the search for inspiral GW

signals from non-spinning compact binaries in the data of ground-based broadband detectors. Further, this work should also be useful in assessing the effects of systematic errors arising from employing inspiral templates from different representations on a GW signal's detectability and parameter estimation with earth-based detectors.

In the literature, there exist gauge-dependent prescriptions for constructing inspiral $h(t)$ that give equal emphasis to both the conservative and the reactive orbital phase evolution, such as the Effective One-Body (EOB) approach [29] and the Semi-Analytic Puncture Evolution (SAPE) [30]. Recall that the conservative Hamiltonian relevant for the EOB scheme is in Schwarzschild-type coordinates, while for SAPE it is in the Arnowitt-Deser-Misner gauge. By contrast, PN-accurate TaylorEt based $h(t)$ is fully gauge-invariant. Therefore, we are pursuing a study, similar to the one presented here, of comparing the effectualness and faithfulness of EOB- and SAPE-based inspiral waveforms vis á vis TaylorEt waveforms. We are also extending the present analysis by including spin effects with the help of a generalized version of fiducial signals and templates detailed in Ref. [31].

Acknowledgments

It is our pleasure to thank Bruce Allen and Gerhard Schäfer for helpful discussions and persistent encouragement. We are grateful for their warm hospitality at Hannover and Jena during various stages of the present study. We would also like to thank B. S. Sathyaprakash for useful observations on the comparison of the different template banks studied here and G. Esposito-Farèse and C. Röver for their careful reading of the manuscript and making helpful suggestions. SB thanks P. Ajith for his explanation of a fast algorithm for computing the fitting factor of a generic template bank and a target signal, and for providing useful comments on this work. This work is supported in part by the NSF grant PHY-0239735 to SB and by grants from DLR (Deutsches Zentrum für Luft- und Raumfahrt) and DFG's SFB/TR 7 "Gravitational Wave Astronomy" to AG and MT, respectively.

[1] C. W. Helstrom, *Statistical Theory of Signal Detection*, 2nd ed. (Pergamon Press, London, 1968).
[2] L. Blanchet, T. Damour, B. R. Iyer, C. M. Will and A. G. Wiseman, Phys. Rev. Lett. **74**, 3515 (1995) [arXiv:gr-qc/9501027].
[3] T. Damour, B. R. Iyer and B. S. Sathyaprakash, Phys. Rev. D **63** (2001) 044023 [Erratum-ibid. D **72** (2005) 029902] [arXiv:gr-qc/0010009].
[4] Information about the LIGO Scientific Collaboration can be found at `http://ligo.org/`.
[5] Details about the Virgo Collaboration can be found at `http://www.virgo.infn.it/`.
[6] Documentation and instructions for using the *LSC algorithm library (LAL)* can be found at `http://www.lsc-group.phys.uwm.edu/lal`. LAL programs are free software that can be availed of by interested users under the terms of the GNU General Public License as published by the Free Software Foundation, `http://www.fsf.org/` .
[7] T. Damour, P. Jaranowski, and G. Schäfer, Phys. Lett. B **513**, 147 (2001); L. Blanchet, G. Faye, B. R. Iyer, and B. Joguet, Phys. Rev. D **65**, 061501(R) (2002); **71**, 129903(E) (2005); L. Blanchet, T. Damour, G. Esposito-Farèse, and B. R. Iyer, Phys. Rev. Lett. **93**, 091101 (2004) and references therein.
[8] L. Blanchet, G. Faye, B. R. Iyer and S. Sinha, arXiv:0802.1249 [gr-qc].
[9] M. Boyle *et al.*, Phys. Rev. D **76**, 124038 (2007) [arXiv:0710.0158 [gr-qc]].
[10] A. Gopakumar, "New Class of Gravitational Wave Templates for Inspiraling Compact Binaries," arXiv:0712.3236 [gr-qc].
[11] T. A. Apostolatos, Phys. Rev. D **52**, 605 (1995).
[12] T. Damour, B. R. Iyer and B. S. Sathyaprakash, Phys. Rev. D **57**, 885 (1998) [arXiv:gr-qc/9708034].
[13] C. Cutler and M. Vallisneri, Phys. Rev. D **76**, 104018 (2007) [arXiv:0707.2982 [gr-qc]].
[14] P. Canitrot, Phys. Rev. D **63**, 082005 (2001).
[15] K. G. Arun, B. R. Iyer, B. S. Sathyaprakash and P. A. Sundararajan, Phys. Rev. D **71**, 084008 (2005). [Erratum-ibid. D **72**, 069903 (2005)] [arXiv:gr-qc/0411146].
[16] F. Pretorius, arXiv:0710.1338 [gr-qc] and references therein.
[17] K.S. Thorne in *300 years of gravity*, edited by S.W. Hawking and W. Israel (Cambridge University Press, Cambridge, England,1987) 330.
[18] A. Gopakumar, M. Hannam, S. Husa and B. Brugmann, "Comparison between numerical relativity and a new class of post-Newtonian gravitational-wave phase evolutions: the non-spinning equal-mass case," arXiv:0712.3737 [gr-qc].
[19] T. Damour, A. Gopakumar and B. R. Iyer, Phys. Rev. D **70**, 064028 (2004) [arXiv:gr-qc/0404128].
[20] M. Tessmer and A. Gopakumar, "Gravitational waves from compact binaries inspiraling along post-Newtonian accurate eccentric orbits: Data analysis implications," arXiv:0712.3199 [gr-qc].
[21] V. Kalogera *et al.*, Astrophys. J. **601**, L179 (2004) [Erratum-ibid. **614**, L137 (2004)] [arXiv:astro-ph/0312101].
[22] R. O'Shaughnessy, C. Kim, T. Frakgos, V. Kalogera and K. Belczynski, Astrophys. J. **633**, 1076 (2005) [arXiv:astro-ph/0504479].

[23] B. J. Owen, Phys. Rev. D **53**, 6749 (1996) [arXiv:gr-qc/9511032].
[24] Since the shape of the LIGO noise PSD is expected to remain mostly unchanged in Enhanced LIGO, we expect the FF numbers and mass-error estimates given here to be roughly applicable for that detector as well.
[25] W. H. Press, W. T. Vetterling,S. A. Teukolsky and B. P. Flannery, *Numerical Recipes in C++: the art of scientific computing*, Cambridge University Press, (2002).
[26] C. Robinson, B. S. Sathyaprakash, and A. S. Sengupta, "A geometric algorithm for efficient coincident detection of gravitational waves," *in preparation*.
[27] B. Abbott *et al.* [LIGO Scientific Collaboration], Phys. Rev. D **77**, 062002 (2008) [arXiv:0704.3368 [gr-qc]].
[28] A. Pai, S. Dhurandhar and S. Bose, Phys. Rev. D **64**, 042004 (2001) [arXiv:gr-qc/0009078].
[29] T. Damour, Int. J. Mod. Phys. A**23**, 1130 (2008) [arXiv:0802.4047 [gr-qc]], and references therein.
[30] A. Gopakumar and G. Schafer, Phys. Rev. D**77**, 104023 (2008) [arXiv:0803.2348 [gr-qc]].
[31] M. Hannam, *et al.*, "Comparison between numerical-relativity and post-Newtonian waveforms from spinning binaries: the orbital hang-up case," arXiv:0712.3787 [gr-qc].

TABLE I: The analytic fits to the one-sided noise power-spectral densities, $S_n(f)$, of LIGO, Virgo and AdLIGO employed in this paper. The expressions for $S_n(f)$ are expressed in terms of $y = f/f_0$, where the "knee frequency" f_0 takes values of 150Hz, 500Hz and 215Hz for the LIGO, Virgo and AdLIGO, respectively. Notice that $S_n(f)$ rises sharply above the seismic cut-off f_s. We drop an overall scale factor from each of the expressions of $S_n(f)$ below as it does not affect our fitting factor studies.

Detector	f_s	$S_n(f)$ (up to an overall scale)
LIGO	40 Hz	$\left\{(4.49\,y)^{-56} + 0.16\,y^{-4.52} + 0.52 + 0.32\,y^2\right\}$
Virgo	20 Hz	$\left\{(6.23y)^{-5} + 2y^{-1} + 1 + y^2\right\}$
AdLIGO	20 Hz	$\left\{y^{-4.14} - 5y^{-2} + \frac{111(1-y^2+y^4/2)}{(1+y^2/2)}\right\}$

TABLE II: Values of the fitting factors and the associated systematic errors in the total mass parameter relevant for the LIGO, Virgo and AdLIGO detectors while employing the TaylorEt approximant at 3.5PN order to model the fiducial inspiral signal. The search templates, extracted from LAL, belong to the TaylorT1 approximant at 3.5PN order in all cases except when the "Detector" is denoted as "AdLIGO-F2"; in the latter case the templates are given by the TaylorF2 approximant at 3.5PN order. The total mass and symmetric mass-ratio parameters of the signal and templates are denoted by (m, η) and (m', η'), respectively. We list m' of the search template that gives the largest match for a given signal. In all the systems below, η' was found to be 0.250 and is, therefore, not listed. The fiducial GW signal and search templates are terminated when the instantaneous GW frequency reaches the value corresponding to the last stable orbit. The low FFs reported in certain cases may be attributed to the fact that we have not allowed η' to go beyond its realistic bound of 0.25. The maximum overlap is always for values of $m' < m$. The numbers below are for the equal-mass case: $q = m_1/m_2 = 1$, i.e., $\eta = 0.25$. It is interesting to note that for small m, Virgo has the worst FF. This owes its cause to a flatter noise PSD at low frequencies which weights the phase difference between the templates and the signal the most there. Also, the FF values of TaylorF2 templates are larger than those of TaylorT1 (computed for comparison only for AdLIGO). This is consistent with the observation in Fig. 2 where the TaylorT4 FF values are also higher than those of TaylorT1. (Recall our speculation that TaylorF2 approximants are essentially stationary phase approximations of TaylorT4 approximants.)

$m_1\ (M_\odot) \equiv m_2\ (M_\odot)$	Detector	FF	$m'\ (M_\odot)$
1.4	AdLIGO-T1	0.96	2.7995
	AdLIGO-F2	0.98	2.8000
	LIGO	0.95	2.7985
	Virgo	0.93	2.7999
3.0	AdLIGO-T1	0.90	5.9924
	AdLIGO-F2	0.94	5.9952
	LIGO	0.94	5.9841
	Virgo	0.87	5.9950
5.0	AdLIGO-T1	0.87	9.9365
	AdLIGO-F2	0.92	9.9404
	LIGO	0.94	9.9117
	Virgo	0.84	9.9740
8.0	AdLIGO-T1	0.87	15.7649
	AdLIGO-F2	0.92	15.7624
	LIGO	0.95	15.6663
	Virgo	0.86	15.8770
10.0	AdLIGO-T1	0.89	19.5718
	AdLIGO-F2	0.90	19.6786
	LIGO	0.96	19.3438
	Virgo	0.89	19.7728
15.0	AdLIGO-T1	0.90	28.8432
	AdLIGO-F2	0.93	29.4024
	LIGO	0.98	28.3201
	Virgo	0.92	29.3476
20.0	AdLIGO-T1	0.92	37.9325
	AdLIGO-F2	0.89	37.5663
	LIGO	0.98	36.8851
	Virgo	0.93	38.6133

TABLE III: Fitting factor values and inherent parameter biases relevant for the LIGO, Virgo and AdLIGO interferometers, for several compact binaries with mass-ratio $q = 1/3$ (i.e., $\eta = 0.1875$)). The other details are as in Table II. We observe that high FFs are always for templates characterized by $m' < m$ and $\eta' \simeq 0.25$. It is clear that the best matched templates are highly biased with respect to their fiducial signals.

m_1 ($M_\odot$) - m_2 ($M_\odot$)	m ($M_\odot$)	Detector	FF	m' ($M_\odot$)	η'
3-9	12	AdLIGO-T1	0.98	10.1630	0.250
		AdLIGO-F2	0.97	10.2269	0.248
		LIGO	0.98	10.1588	0.250
		Virgo	0.97	10.1596	0.250
4-12	16	AdLIGO-T1	0.97	13.5519	0.250
		AdLIGO-F2	0.98	13.5704	0.250
		LIGO	0.98	13.5078	0.250
		Virgo	0.97	13.5522	0.250
5-15	20	AdLIGO-T1	0.96	16.9127	0.250
		AdLIGO-F2	0.97	16.9609	0.250
		LIGO	0.98	16.8320	0.250
		Virgo	0.97	16.9299	0.250
7-21	28	AdLIGO-T1	0.96	23.6070	0.250
		AdLIGO-F2	0.96	23.7107	0.250
		LIGO	0.99	23.4532	0.247
		Virgo	0.97	23.6543	0.250
10-30	40	AdLIGO-T1	0.98	33.5956	0.250
		AdLIGO-F2	0.95	33.8244	0.249
		LIGO	0.98	35.4216	0.208
		Virgo	0.98	33.6106	0.250

TABLE IV: Fitting factor values, relevant for the LIGO, Virgo, and AdLIGO, for several compact binaries having mass ratio $q = 1/4$ or $\eta = 0.16$. The other details are as in Table II, and our conclusions are also similar to those reported in Table III. Additionally, it is interesting to observe that across both Table III and the current table, as the total mass of the system is increased in LIGO, the bias in η' there appears to decrease noticably. This is because LIGO has a higher f_s than the other detectors considered here (see Table I). Correspondingly, the number of in-band cycles is considerably reduced in it for higher mass, to the extent that tuning only one parameter, m' , in LIGO suffices to attain higher FFs.

m_1 ($M_\odot$) - m_2 ($M_\odot$)	m ($M_\odot$)	Detector	FF	m' ($M_\odot$)	η'
3-12	15	AdLIGO-T1	0.97	11.7544	0.246
		AdLIGO-F2	0.97	12.2512	0.228
		LIGO	0.99	11.9641	0.238
		Virgo	0.95	11.7448	0.246
4-16	20	AdLIGO-T1	0.98	15.5198	0.250
		AdLIGO-F2	0.97	16.0009	0.237
		LIGO	0.99	15.5188	0.250
		Virgo	0.98	15.5213	0.250
5-20	25	AdLIGO-T1	0.98	19.4193	0.250
		AdLIGO-F2	0.96	20.2636	0.231
		LIGO	0.99	20.3615	0.224
		Virgo	0.99	19.4180	0.250
28-7	35	AdLIGO-T1	0.96	27.2169	0.250
		AdLIGO-F2	0.96	27.6552	0.243
		LIGO	0.98	28.7005	0.217
		Virgo	0.98	27.2233	0.250
8-32	40	AdLIGO-T1	0.98	32.0353	0.234
		AdLIGO-F2	0.95	32.0962	0.235
		LIGO	0.98	35.9969	0.167
		Virgo	0.98	31.9093	0.236

TABLE V: The recomputed FF values for AdLIGO for compact binaries studied in Table II. Unlike in that table, here we allowed the symmetric mass-ratio parameter of the templates to vary beyond the physically allowed range, and up to $\eta' = 0.35$. As shown below, doing so improves the FFs to be higher than or equal to the desirable lower-limit of 97%. However, this gain comes at the cost of high biases in estimated masses and, possibly, an increased noise contribution to the detection statistic.

m_1 $(M_\odot)$	FF	m' $(M_\odot)$	η'
1.4	0.99	2.7350	0.260
3	0.99	5.5939	0.288
5	0.99	8.8575	0.308
8	0.99	13.4103	0.341
10	0.98	16.5826	0.348
15	0.97	24.7678	0.350
20	0.97	32.6322	0.350

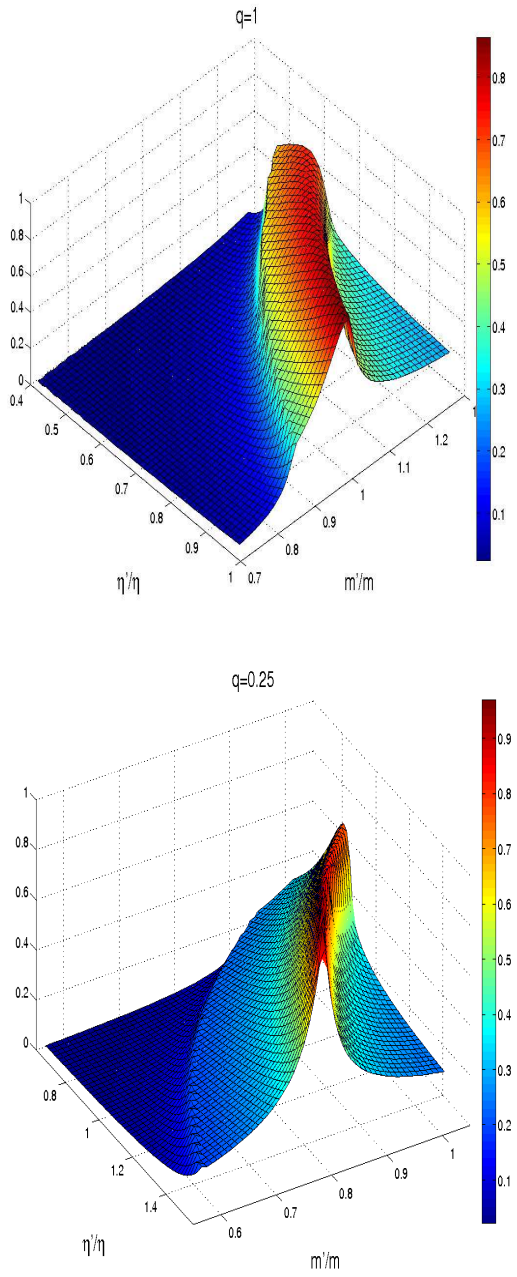

FIG. 1: The plots display the match M (see Eq. 10) [12] as a function of the parameters (m', η') of the search templates. The plot axes are η'/η and m'/m, where (m, η) are the values of the TaylorEt signal parameters. For the equal-mass case ($q = 1$), the match keeps rising as η' is increased and attains its global maximum in the unphysical region $\eta' > 0.25$. In the $q = 1/4$ plot, the maximum value of M is around $\eta' \sim 0.25$, which is much larger than the signal parameter value of $\eta = 0.16$. The maximum match remains fairly high, at more than 0.95, on certain crests of the ridges.

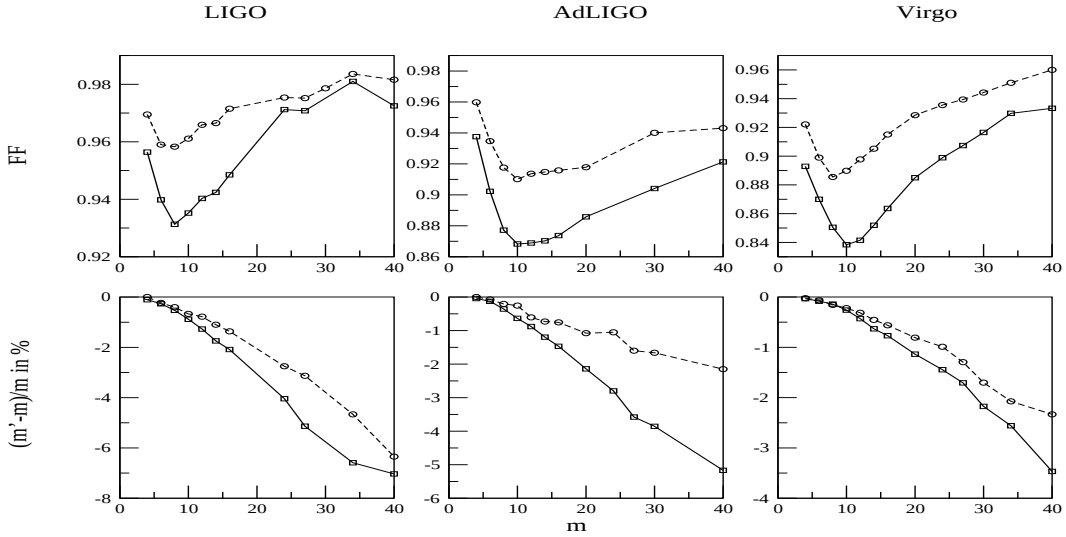

FIG. 2: A collection of plots that summarizes a set of results from our fitting-factor studies involving the TaylorEt, TaylorT1/TaylorT4 approximants at 3.5PN order for equal-mass binaries. The first row provides plots of FF against the total mass of the inspiral signals and the second row shows fractional error (in percentage) in the estimated total-mass values as a function of the signal's total-mass. The thick and dashed lines denote results for the TaylorT1 and TaylorT4 approximants, respectively. For high mass binaries, we observe high biases in the m' values. Above, we do not provide η' versus m plots as the best matched filters always have $\eta' \simeq 0.25$.

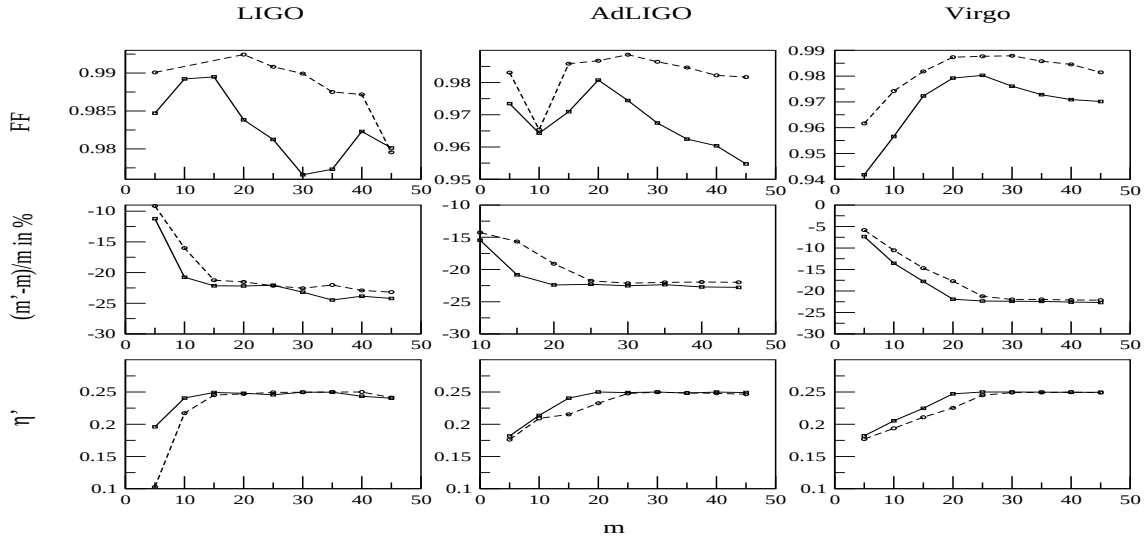

FIG. 3: A set of plots summarizing our fitting-factor and parameter estimation results for the TaylorEt, TaylorT1 approximants at 3.5PN order for compact binaries having $q = 1/4$. The first two rows show plots analogous to those presented in Fig. 2. The third row shows plots of η' versus m. (Note that $\eta = 0.16$ in all these plots.) Here too the thick and dashed lines are for the TaylorT1 and TaylorT4 approximants, respectively. We clearly observe substantially higher biases for η' that for m' values and in most cases, the best matched templates always have $\eta' \simeq 0.25$.